Feasibility study of a rail vehicle damper fault detection by artificial neural networks

Indexed by:
Web of Science Group

Rafał Melnik[a], Seweryn Koziak[b], Ján Dižo[c], Tomasz Kuźmierowski[a], Ewa Piotrowska[a]

[a] Lomza State University of Applied Sciences, Faculty of Computer Science and Technology, Akademicka 1, Lomza, Poland
[b] Warsaw University of Technology, Faculty of Transport, Koszykowa 75, Warsaw, Poland
[c] University of Žilina, Faculty of Mechanical Engineering, Univerzitná 8215/1, Žilina, Slovakia

Highlights

- Primary suspension damper failures affect vehicle dynamics.
- Detection of damping reduction is based on the analysis of acceleration signals in frequency domain.
- Artificial neural networks of different number of hidden layers were applied to accelerations' PSDs.
- ANNs training process was a difficult task, resulting in fault detection rate below 63%.

Abstract

The aim of the study was to investigate rail vehicle dynamics under primary suspension dampers faults and explore possibility of its detection by means of artificial neural networks. For these purposes two types of analysis were carried out: preliminary analysis of 1 DOF rail vehicle model and a second one - a passenger coach benchmark model was tested in multibody simulation software - MSC.Adams with use of VI-Rail package. Acceleration signals obtained from the latter analysis served as an input data into the artificial neural network (ANN). ANNs of different number of hidden layers were capable of detecting faults for the trained suspension fault cases, however, achieved accuracy was below 63% at the best. These results can be considered satisfactory considering the complexity of dynamic phenomena occurring in the vibration system of a rail vehicle.

Keywords

rail vehicle, damper, suspension, fault detection, neural networks

1. Introduction

The problem of vehicle-rail interaction has been an important issue practically since the beginning of rail transport. The implementation of suspension in the design of the first locomotives and wagons made it possible to increase speeds, passenger comfort and freight weight, what in turn began improving running characteristics and reducing track loading. Over the years, rail vehicle suspensions have become increasingly sophisticated mechanical systems that allow the wheelsets to be properly guided in the track, ensure good running smoothness in tracks with irregularities along with transmitting traction and braking forces. The properties of the suspension have a major influence on the dynamic behavior which is examined particularly rigorously for approval testing of the vehicles before gaining authorization for placing on the market. Improper selection of stiffness and damping, as well as incorrect geometric sizing of constraint elements may result in the generation of excessive lateral contact forces, high values of derailment quotient and unacceptable accelerations. Consequently, such a vehicle will not only be unsafe for the passengers or the transported goods, but may also have a destructive effect on the tracks. Suspension components are subject to wear and random failure, e.g. due to overloading, degrading ride comfort, dynamic performance and in extreme conditions leading to derailment [28]. Not all types of damages to suspension components may be noticed during routine and scheduled inspections, such as broken coil/leaf springs and their corrosion, cracks of rubber-metal spring, leaking dampers, mounting freeplays, etc. Especially, due to the complexity of a hydraulic damper design its condition can be particularly difficult to assess when there are no operating fluid leaks or other external damages. Thus the only reliable way to determine the condition of a possibly faulty hydraulic damper is to examine it on a special test stand and compare its characteristics to a model-specific benchmark. These characteristics usually include:

(*) Corresponding author.
E-mail addresses: R. Melnik (ORCID: 0000-0003-2900-784X) rmelnik@ansl.edu.pl, S. Koziak (ORCID: 0000-0002-6922-3574) seweryn.koziak@pw.edu.pl, J. Dižo (ORCID: 0000-0001-9433-392X) jan.dizo@fstroj.uniza.sk, T. Kuźmierowski (ORCID: 0000-0002-6090-8948) tkuzmierowski@ansl.edu.pl, E. Piotrowska (ORCID: 0000-0003-3163-0753) epiotrowska@ansl.edu.pl

maximum damping force at tension and compression, as well as hysteresis loop, damping force vs working stroke. Not all rolling stock operators or repair facilities possess this type of equipment, what may result in the defective component only being replaced during an inspection in which the bogie undergoes a major repair. Implementation of condition monitoring is regarded as a possible way of detecting suspension faults of the rail vehicles' running gears. Such the systems may support preventive maintenance systems leading to increase of the vehicles' reliability, availability, safety and allow prediction of future technical condition.

The aim of the presented study was to investigate the feasibility of damper faults detection by means of artificial neural networks (ANN) of different number of hidden layers applied solely to vibration signals' spectra obtained from multibody simulation. The fault detection method based on ANNs could be further implemented in the condition monitoring system. Moreover, the paper analyses numerically the effects of loss of damping on rail vehicle dynamics.

2. Rail vehicles' suspension fault detection methods – state of the art

Rail vehicle suspension fault detection methods are part of a broad Fault Detection and Idnetification (FDI) techniques and have been intensively developed since mid-2000s. Most of the literature on the subject matter proposes model based methods supported with a state observer. Essentially those methods involve comparing the actual system's measured response to an input with the response obtained (estimated) from the mathematical model with predefined geometric, inertial, stiffness and damping parameters. The difference between those two responses, the so-called residual, is generated and on the basis of its value the system's condition is inferred. Some of the earliest papers on the model-based methods were by Li and Goodall. They made use of Kalman filter (KF) [20] and Rao-Blackwellised Particle Filter [20] in order to estimate the state of the plant represented by a matrix of suspension and inertial parameters of the second order differential equations governing vehicle dynamics. Kalman filter was also used by Tsunashima et al. in the multiple-model approach [9]. Wei et al. applied KF to generate the residuals for fault diagnosis and processed the results using Dempster-Shafer evidence theory [35]. Another version of KF - cubature Kalman filter – has been recently implemented for suspension fault detection by Zoljic-Beglerovic et al. [43]. Liu et al. [22] presented a model-based strategy for condition monitoring of suspensions in a railway bogie. This approach is based on the recursive least-square (RLS) algorithm focusing on the 'Input-output' model.

The model-based methods require aforementioned vehicle parameters. Already at the modelling stage, simplifications, including linearization, are introduced that may limit the effectiveness of these methods. In addition, access to the required parameters could be problematic as the vehicle and components manufacturers may not provide such detailed information. In parallel to the model-based methods a signal processing approach has also been developed. Mei and Ding [24] presented a new technique evaluating dynamic interactions between different vehicle modes caused by component failures in the suspension system. Wei et al. [36] considered vertical

damper fault and vertical spring fault detected by the Dynamical Principle Component Analysis (DPCA) and Canonical Variate Analysis implemented on acceleration signals acquired from simulation. Sorribes-Palmer et al. [32] developed a fault detection technique which is based on the acoustic emissions variation due to structural modal coupling changes in the presence of faulty components. Sakellariou et al. [30] trained FDI unit basing on measurement signals obtained from the physics-based vehicle model in the baseline phase, subsequently it achieved fault diagnosis in the inspection phase using the advanced functional model based method (FMBM). Furthermore, they implemented stochastic ARX-type models to represent a system in a faulty state. Fault detection by analysis of distance in a diagnostic space made up of selected statistical parameters of acceleration signals is presented in [26]. Dumitriu [4] investigated the possibility of developing a new method for fault detection of a damper in the primary suspension of the railway vehicle, based on the analysis of the vertical vibration's response of the bogie, regarding the RMS accelerations measured/simulated in four reference bogie points. Also Dumitriu in the previous work [5] proposed a method to detect the failure of the damper in the primary suspension of the rail vehicle, based on the analysis of cross-correlation of the vertical accelerations measured on the bogie frame against the two axles.

Due to successful operation in various branches of engineering, machine learning techniques have also been applied to the problem of suspension fault detection. Hu et al. [12] adopted the deep neural network to recognize faults in bogies: failure of the lateral damper, anti-yaw damper, air springs and combination of failures of these elements. Karlsson et al. [15] computed frequency response functions among acceleration signals in the carbody, bogie frames and axles, which served as fault indicators, fed to the classification algorithms – the linear Support Vector Machine and 1-Nearest-Neighbour. Ankrah [1] built a supervised machine learning model to predict faulty and healthy state of the suspension system components, based on support vector machine (SVM). They also developed a new SVM model to predict faults on the test data containing acceleration obtained from simulation scenarios. Dai et al. [3] used neural network model that describes the characteristics of the hydraulic damper, such as oil leakage, the internal friction force and the percentage of entrapped air in oil. The responses and the dynamic parameters of the hybrid neural network model were calculated and compared with the experimental results by considering various exciting amplitudes and frequencies. A 1D convolution network-based fault diagnostic method for high speed train suspension systems was designed by Ye et al [39]. In order to improve the robustness of the method, a Gaussian white noise strategy for immunity to track irregularities and an edge sample training strategy for immunity to wheel wear were proposed. Ren et al. [29] considered detection of lateral and yaw damper failures by means of a novel 1D-ConvLSTM time distributed convolutional neural network (CLTD-CNN). Wu et al. [38] proposed synchrony group convolutions to construct a fault diagnosis scheme for we propose synchrony group convolutions for a high-speed train bogie. The examined five categories of faults: air spring fault, wheel-box spring fault, lateral damper fault, yaw damper fault, and vertical damper fault.

3. Preliminary analysis of damper failure

The general effect of damping decrease is firstly demonstrated by analysing frequency response of the 2-axle HSFV1 goods wagon. This type of wagon has been chosen due to its running gear with a single suspension-level and the use of hydraulic dampers which are typically installed in passenger vehicles rather than in goods wagons. The bogie-less design of the running gear allows representing this type of wagon by means of a simple 1 DOF quarter vehicle model, depicted in Fig. 1. The model consists of quarter of a body mass $m_b = 7500 \, kg$ (unloaded) connected with half of a wheelset of mass $m_w = 1196 \, kg$ by means of a spring and a dashpot with constants $k = 4.1 \cdot 10^6 \, N/m$ and $c = 28 \cdot 10^3 \cdot Ns/m$ respectively [40].
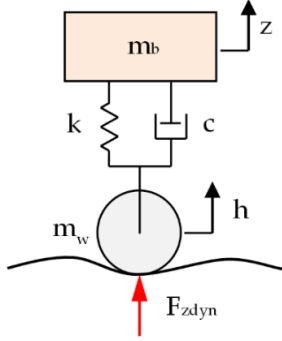

Fig. 1. Quarter rail vehicle model (bogie-less).

Frequency response of the body mass acceleration (acceleration gain) is derived analytically basing on the equation of motion (1). The notation is adopted from [27].

$$m_b \ddot{z} + c \dot{z} + k z = c \dot{h} + k h \quad (1)$$

Harmonic excitation h of the wheel mass mw and response z of body mass mb are given by equation (2):

$$h = \hat{h} e^{j \omega t}, z = \hat{z} e^{j \omega t} \quad (2)$$

where h hat and z hat are complex amplitudes. Substituting (2) into (1) yields:

$$(-m_b \omega^2 + jc\omega + k)\hat{z} = (jc\omega + k)\hat{h} \quad (3)$$

thus body acceleration gain is:

$$\frac{\ddot{\hat{z}}}{\hat{h}} = \omega^2 \frac{jc\omega + k}{-m_b \omega^2 + jc\omega + k} \quad (4)$$

Wheel dynamic load F_{zdyn} (Fig. 1), neglecting wheelset and body weight, is:

$$F_{zdyn} = m_w \ddot{h} + m_b \ddot{z} \quad (5)$$

hence wheel dynamic load gain is expressed as:

$$\frac{\hat{F}_{zdyn}}{\hat{h}} = -m_w \omega^2 - m_b \omega^2 \frac{jc\omega + k}{-m_b \omega^2 + jc\omega + k} \quad (6)$$

The damper failures in the considered case are expressed as a percentage of nominal damping c_{nom}, i.e. 75% c_{nom}, 50% c_{nom} and 10% c_{nom}. It is evident that, if excitation frequency matches mass' natural frequency, body acceleration and wheel dynamic load abruptly increase, especially for $c = 10\% \, c_{nom}$. Unfortunately, for the purpose of fault detection, frequency response of vehicle with $c = 75\% \, c_{nom}$ and 50% c_{nom} are much less distinguishable from the response of the vehicle in healthy condition (Fig. 1a). The 90% decrease in damping has also its negative effect on track since wheel dynamic load gain is heavily increased (Fig. 2b).

In normal operation excitation frequency is a combination of vehicle variable speed and different wavelengths of rails' irregularities, as well as track geometry and other track imperfections (e.g. variable track vertical stiffness). Furthermore, in a real rail vehicle other factors contribute to the magnitude of frequency response, e.g.: inertial forces, vibration coupling of different vehicle's masses, wheelsets' out-of-roundness, variable vehicle mass and aerodynamic loads. Thus it is difficult to develop a suspension fault detection method for the condition monitoring system that could deal with variable operating conditions and would be robust to the random disturbances causing dynamic responses of the vehicle as if its suspension elements were damaged.

4. Full rail vehicle model

Simulation analysis of full rail vehicle dynamics was carried out in a multibody environment MSC.Adams with use of rail package VI-Rail. For the purpose of the study a benchmark model of a typical 4-axle passenger coach was chosen [13]. The built model belongs to the group of the so-called low-frequency models. It is assumed that the upper limit of the low-frequency vibration range is 30–50 Hz. Inertial objects of the vehicle performing low-frequency vibrations behave as rigid bodies, which allows us to assume the rigidity of the main components of the vehicle model – the body, bogie frames and wheelsets. Those elements are connected by linear, massless springs, dampers and joints. Forces from the bogie are transmitted to the carbody via traction rod. The model does not have yaw dampers.
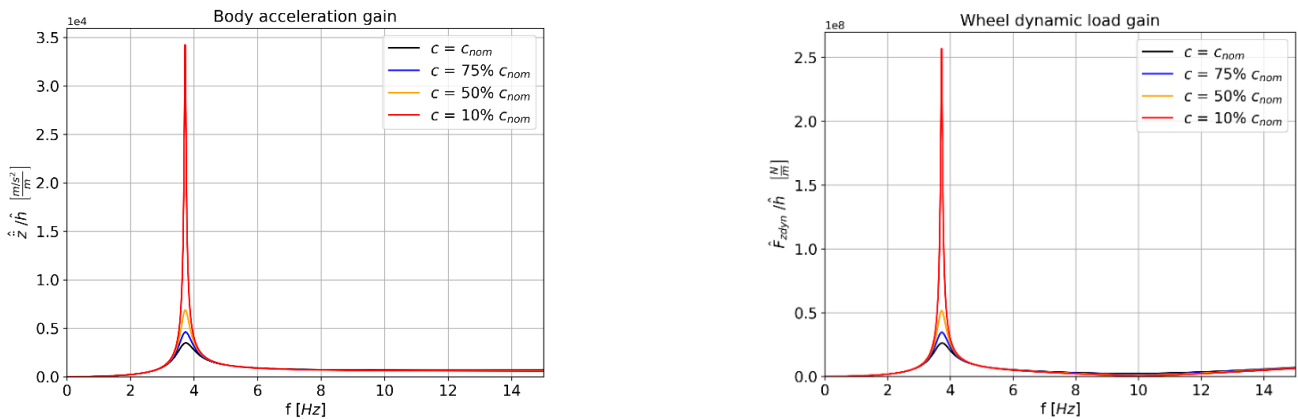

Fig. 2. Body acceleration gain (a) and wheel dynamic load gain (b) for different excitation frequencies and damper conditions. The main parameters of the model are presented in Tab. 1.

Tab. 1. Main passenger coach model parameters.

Parametr	Value
Geometry and masses	
Bogie pivot spacing	19 m
Bogie wheelbase	2.56 m
Wheel radius	0.46 m
Wheelset mass	1813 kg
Bogie mass	2615 kg
Body mass	32000 kg
Primary suspension stiffness	
Longitudinal	31391 kN/m
Lateral	3884 kN/m
Vertical	1220 kN/m
Primary suspension damping	
Longitudinal damping	15 kNs/m
Lateral damping	2 kNs/m
Vertical damping	4 kNs/m
Secondary suspension stiffness	
Longitudinal stiffness	160 kN/m
Lateral stiffness	160 kN/m
Vertical stiffness	430 kN/m
Traction rod longitudinal stiffness (one per bogie)	5000 kN/m
Secondary suspension damping	
Longitudinal damping (traction rod)	25 kNs/m
Lateral damping	32 kNs/m
Vertical damping	20 kNs/m

The position of the rigid body's mass centre is described by position vector p of three coordinates x, y, z, of the Cartesian reference frame:

$$p = \begin{bmatrix} x \\ y \\ z \end{bmatrix} \qquad (7)$$

Orientation of the body is described by means of three Euler angles: φ, χ, ψ consistent with the rotation sequence 3-1-3:

$$\varepsilon = \begin{bmatrix} \varphi \\ \chi \\ \psi \end{bmatrix} \qquad (8)$$

The set of generalized coordinates associated with the i-th body is defined in ADAMS environment by vector q:

$$q_i = \begin{bmatrix} p_i \\ \varepsilon_i \end{bmatrix} \qquad (9)$$

Joints connecting the solids are treated as constraints, which are imposed on generalized coordinates from q_i to q_n. Taking into account time dependency of the considered multibody system, the constraints formula is:

$$\Phi = (q, t) = 0 \qquad (10)$$

ADAMS software generates automatically and solves equations of motion for individual inertial elements of a complex mechanical system. The dynamic behaviour of the elements of the system is described in ADAMS environment by means of a system of differential-algebraic equations derived from the Euler-Lagrange formalisms presented in a general form [23]:

$$\frac{d}{dt}\left(\frac{\partial L}{\partial \dot{q}}\right) - \frac{\partial L}{\partial q} + \Phi_q^T \lambda = Q \qquad (11)$$

where:

q - vector of generalized coordinates;
L - Lagrangian (difference of kinetic and potential energy: $L = T - V$);
Φ_q - Jacobian matrix of constraints;
λ - vector of Lagrange multipliers;
Q - vector of external forces.

Systems of nonlinear differential equations are solved by the ADAMS solver numerically, mainly using the Newton-Raphson method. The method of creep-force computation, implemented in the simulation software, is based on Kalker's FASTSIM algorithm [14]. The code uses actual wheel and rail profile and computes the actual contact kinematics at each simulation step.

5. Track models

The tracks of two different geometries have been used in the study, namely *S*-shaped curves and the model of the experimental track in Żmigród (Poland) which belongs to the Railway Institute [10].

The specific *S*-shaped curves consist of two inverse curves of radii $R = 150$ m and total length of ca. 100 m. This kind of track is used during the acceptance tests [6] for investigating safety against derailment under longitudinal compressive forces within trains.

The model of the experimental track in Żmigród has total length of 7725 m. Its longitudinal profile is shown in Table 2 and its plan is depicted in Fig. 3.

Vertical stiffness of both track models was assumed as infinite and rail profile was standard, unworn UIC60.

Tab. 2 Experimental track profile.

| Distance [m]	Description
0056.595 - 0186.595	transition curve
0186.595 - 1754.47	R=600 m, cant 0.15 m
1754.47 - 1884.47	transition curve
1884.47 - 1938.97	tangent section
1938.97 - 2018.97	transition curve
2018.97 - 2052.53	R=800 m, cant 0.09 m
2052.53 - 2132.53	transition curve
2132.53 - 2159.93	tangent section
2159.93 - 2261.13	transition curve
2261.13 - 2410.02	R=700 m, cant 0.115 m
2410.02 - 2511.22	transition curve
2511.22 - 3045.863	tangent section
3045.863 - 3165.863	transition curve
3165.863 - 6347.747	R=900 m, cant 0.1 m
6347.747 - 6467.747	transition curve
6467.747 - 7725.00	tangent section
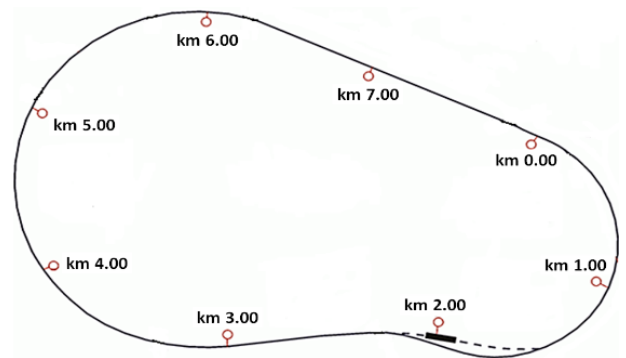
Fig. 3. Experimental track plan.

Additionally, track irregularities were implemented in both track models. The height of the irregularities was generated from power spectral densities for vertical (S_{zz}) and lateral (S_{YY}) directions [7] according to the following formulas (12, 13):

$$S_{zz} = \frac{A_v \Omega_c^2}{(\Omega^2 + \Omega_r^2)(\Omega^2 + \Omega_r^2)} \qquad (12)$$

$$S_{YY} = \frac{A_A \Omega_c^2}{(\Omega^2 + \Omega_r^2)(\Omega^2 + \Omega_r^2)} \quad (13)$$

where:
Ω_c = 0.8246 rad/m
Ω_r = 0.0206 rad/m
A_v = 1.08 10^{-6} m rad
A_A = 6.125 10^{-7} m rad

The generated irregularity waveform for each rail and direction consisted of 200 harmonics. Minimum wavelength was set to 5 m, whereas maximum to 1000 m, which determine the upper and the lower frequency limit of the PSD function respectively. Statistical values of the irregularities are presented in Tab. 3 and Tab. 4. According to the former classification of track quality levels described in UIC 518 leaflet [33], S-shape curve falls into good quality (QN1) in terms of absolute peak values for tracks with allowable speed ⩽ 80 km/h. However, due to standard deviation of height of the irregularities, it can be classified as medium quality (QN2). Since the permissible speed on the second track is 160 km/h, its quality can be assessed as medium (QN2) considering the peak values of the height of the irregularities, while in terms of standard deviation, the quality of the track is poor (QN3).

Tab. 3 Height of the track irregularities in S-shaped curves.

Height (mm)	Left Y	Left Z	Right Y	Right Z
Min.	-5.28	-7.18	-3.31	-8.43
Max.	3.32	8.58	5.28	6.80
Standard dev.	2.58	4.14	2.58	3.70

Tab. 4 Height of the track irregularities in experimental track model.

Height (mm)	Left Y	Left Z	Right Y	Right Z
Min.	-10.10	-15.70	-11.00	-15.20
Max.	11	14.7	10.10	15.30
Standard dev.	3.06	4.44	3.06	4.28

6. Rail vehicle dynamic behavior under primary suspension dampers faults

6.1. Damper damage effect on rail vehicle dynamics

Suspension damages or variation of suspension parameters and their effect on dynamic behavior of a rail vehicle have been investigated previously in various studies. In [25] the authors presented analysis of acceleration signals obtained during experimental tests of rail vehicles with introduced faults of primary and secondary suspension. Stationary tests of a wagon with leaf spring damages and analyses of recorded acceleration signals are described in [19]. The study in [34] focused on simulation of dynamic responses of a rail vehicle with nonlinear secondary suspension damper model differentiating its parameters. Numerical simulations of a rail vehicle with stochastic failure of dampers were performed for failure effects analysis on dynamical performance in [41].

This section examines the dynamic behavior of the vehicle as a result of a 90% reduction in damping in the vertical direction at both wheels of the first wheelset. For that purpose simulation tests have been carried out in the S-shaped track. Initial speed of the vehicle was 50 km/h which can be considered as dangerous for the adopted track geometry. The excessive speed was chosen because the viscous damper generates a force that depends on the velocity of displacement of the piston rod. In the case of sudden changes in load acting on the vehicle, the effect of the

damping is more noticeable compared with riding at lower speeds and in curves of greater radii, when the loads acting on the vehicle are much less significant. The adopted measures of vehicle's dynamic behavior are the following quantities: lateral forces, Y/Q ratio and wear number, all related to the left and right wheel of the first wheelset. Quotient of lateral force to vertical force is calculated basing on Nadal's criterion and assesses the risk of flange climb derailment [16, 17]. Formula (14) is derived from the static equilibrium of wheel's lateral force Y and vertical force Q acting on a rail (Fig. 4).
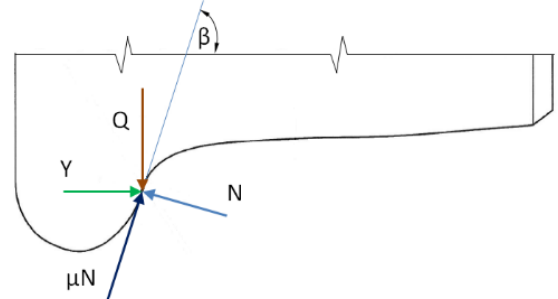

Fig. 4. Forces acting on a wheel flange.

$$\frac{Y}{Q} = \frac{\tan\beta - \mu}{1 + \mu\tan\beta} \quad (14)$$

where: β - flange angle, μ - friction coefficient between wheel and rail

The wear number (W_n) is based on T-gamma energy model, whose assumption is the proportional relationship between the amount of worn material and the dissipated energy in the wheel-rail contact zone. It is equal to the sum of products of wheel-rail longitudinal F_x and lateral F_y creep forces, and wheel creepages γ_x and γ_y (15):

$$W_n = F_x \gamma_x + F_y \gamma_y \quad (15)$$

The result of the simulation in the S-curve are presented in the form of percentage changes of minimum, maximum, standard deviation and mean value of the measured quantities (Fig. 5 - Fig. 7). In this specific track, the measured quantities show changes due to damping reduction. For the left wheel, the mean values are increased, while for the right wheel they are reduced. The variations of extreme values (min, max) are more apparent, however, they do not contribute much in the entire ride, since the changes of mean values are lower than the changes of the extremes.
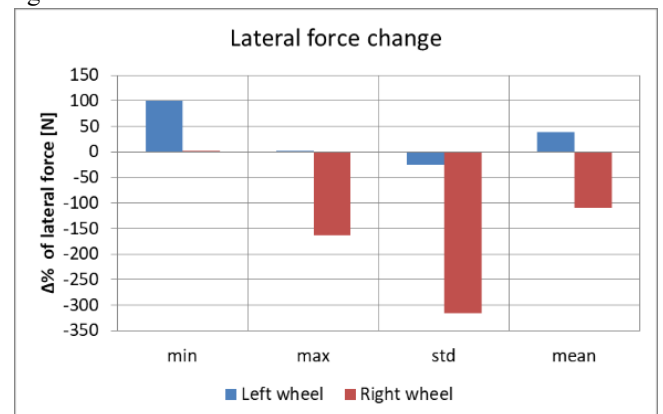

Fig. 5. Percentage change of lateral force on the left and right wheel of the first wheelset in the S-shaped curve, v = 50 km/h.
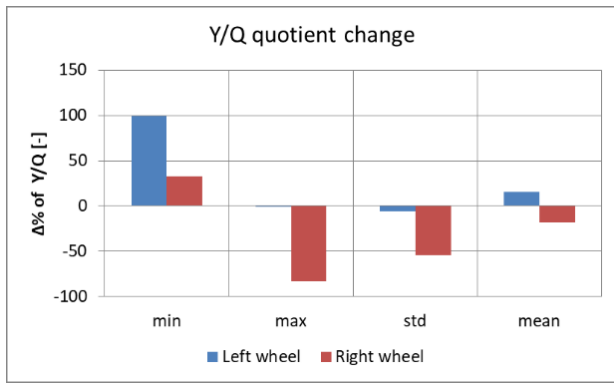
Fig. 6. Percentage change of Y/Q quotient on the left and right wheel of the first wheelset in the S-shaped track, $v = 50$ km/h.
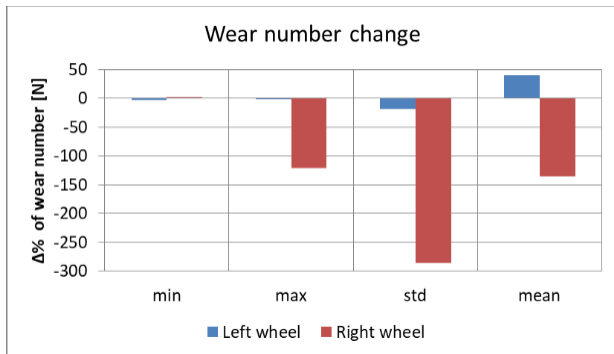

Fig. 7. Percentage change of wear number on the left and right wheel of the first wheelset in the S-shaped track, $v = 50$ km/h.

6.2. Simulation on the experimental track

Simulation of the passenger coach dynamics on the experimental track model was carried out in order to provide input data for training the artificial neural network. The tests were performed for different configurations of primary suspension damper failures which are placed in Tab. 5 as simulation scenarios. The convention of identifying faults is: #X, where # is a number referring to the wheelset, X refers to left of right side of the vehicle. Damping values in scenario 8 has been chosen arbitrary. The simulation tests were performed for two speed values: 100 km/h and 160 km/h - maximum permissible speed on the experimental track.

Tab. 5 Simulation scenarios, L - left wheel, R - right wheel.

Scenario	Faults
Sc1	All dampers nominal
Sc2	1L - 75% c_{nom}
Sc3	1L - 50% c_{nom}
Sc4	1L - 10% c_{nom}
Sc5	1L, 1R - 75% c_{nom}
Sc6	1L, 1R - 50% c_{nom}
Sc7	1L, 1R - 10% c_{nom}
Sc8	1L - 50% c_{nom} 1R - 75% c_{nom} 2L - 50% c_{nom} 2R - 10% c_{nom} 3L - 75% c_{nom} 3R - 50% c_{nom} 4L - 10% c_{nom} 4R - 10% c_{nom}

Acceleration signals were recorded, in vertical and lateral direction, in the points of the vehicle specified in the railway standard [6], i.e.:

- axleboxes,
- bogie frames - above wheels,
- carbody - above bogie's center.

which contribute to the total of 36 channels.

Due to the various track geometry, for the purpose of the analysis, the recorded data were divided into parts according to the following sections covering the distances:

- section 1: 0 - 1861 m,
- section 2: 1862 - 2141 m,
- section 3: 2142 - 2527 m,
- section 4: 2528 - 3031 m,
- section 5: 3032 - 6483 m,
- section 6: 6484 - 7725 m.

Prior to analysing the acceleration signals, it is first important to study the effect of damping detuning on the eigenvalues of the wagon model. This analysis determined the sensitivity of the model to the change of damping parameters, and thus the degree of difficulty of suspension damage detection. In this case the considered damage was 90% reduction (c = 10% c_{nom}) of damping of both wheels of the first wheelset. As it can be seen in Fig. 8, values of the real part of eigenvalues (corresponding to damping) are only slightly affected by dampers faults, however, the number of eigenvalues in the case of faulty dampers increased by 1 (68 vs 69). This fact may indicate occurrence of a new mode shape due to vibrations coupling. Apart from that extra mode shape, all other eigenvalues of faulty vehicle practically overlap eigenvalues of the vehicle in nominal condition, thereby detection of suspension faults would be very difficult basing on dynamic responses of the model.
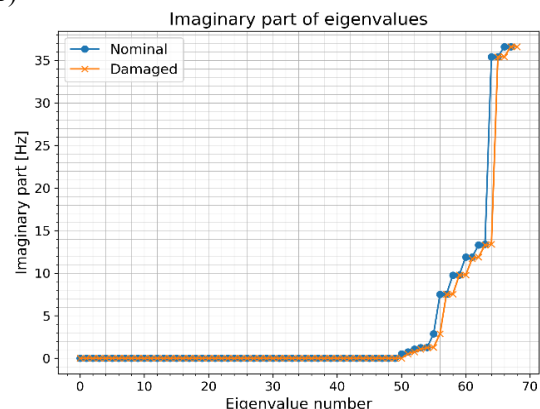
a)
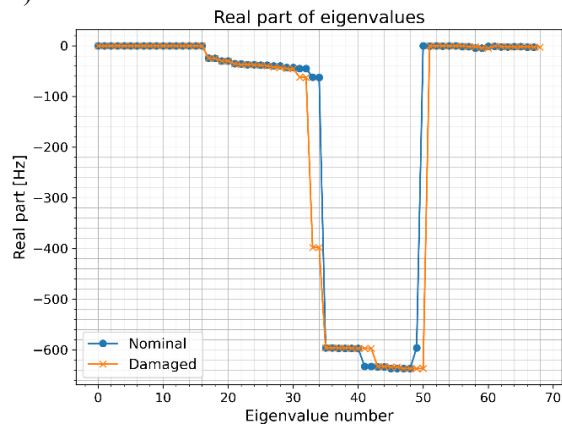
b)

Fig. 8. Rail vehicle model's eigenvalues real part (a) and imaginary (positive values) part (b).

Analysis of acceleration signals obtained from simulation was carried out on the basis of estimated power spectral densities (PSD) by means of Welch's periodograms [31, 37]. Fig. 9 - Fig. 14 present PSD of the recorded acceleration signals on the left axlebox of the first wheelset, on the bogie frame above the left wheel of the first wheelset and on the carbody above the center of the leading bogie. The simulation results presented herein correspond to the same fault as in the case of eigenvalues analysis. It can be concluded on the basis of these figures that distribution of PSD values changes over the entire spectrum and the effect of damping reduction is much more difficult to extract compared with 1 DOF model. Due to the complexity of the full rail vehicle model, vibration modes couplings occur, impeding diagnostic inference. However, damping detuning in vertical direction of primary suspension has virtually no effect on vibrations recorded on the carbody in the analysed model. Another feature making damage detection difficult is the low sensitivity of the vehicle model to damping detuning. From Fig. 9-10 and Fig. 12-13 it is evident that acceleration signals differ substantially due to speed and considered track section rather than as a result of damping decrease. For instance, the PSD values of the acceleration signals recorded on the bogie frame for $v = 160$ km/h (Fig. 13a and Fig. 13b) differ by an order of magnitude compared to the PSD values of the signals recorded for $v = 100$ km/h (Fig. 10a and Fig. 10b).

This marginal differences of PSD values from nominal and damaged vehicle lead to the conclusion that fault detection method based on the analysis of signal's statistical parameters values only (including PSD values) will not be fully effective.
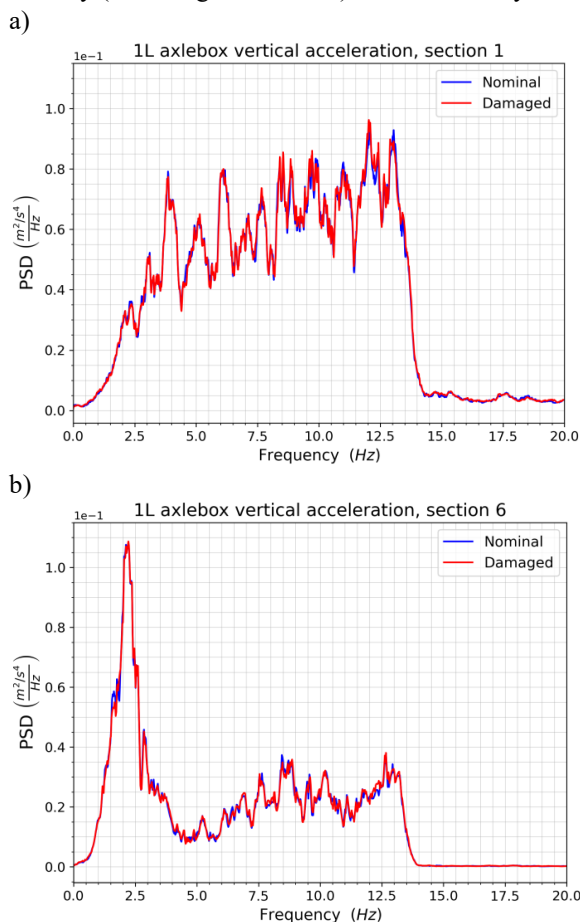
a)

b)

Fig. 9. Axlebox vertical acceleration obtained from section 1 (a) and section 6 (b), v = 100 km/h.
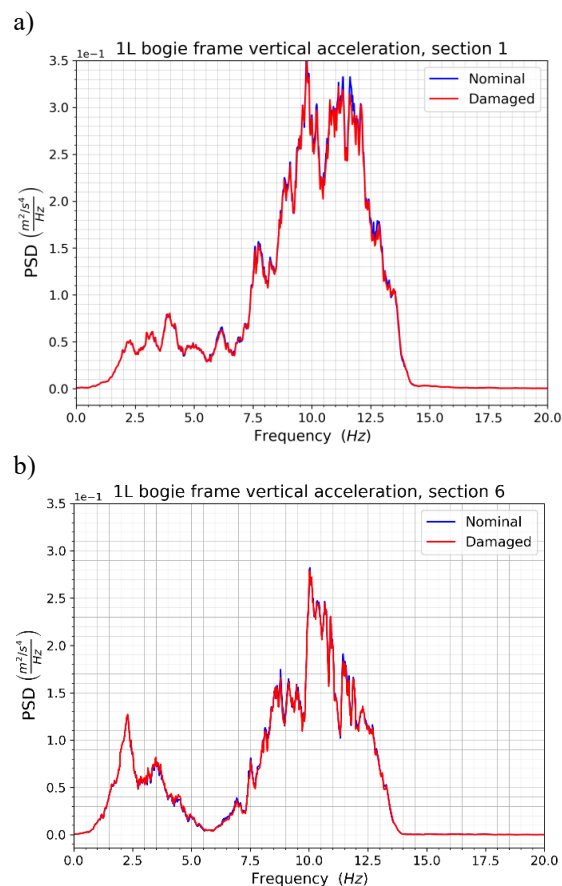
a)

b)

Fig. 10. Bogie frame vertical acceleration obtained from section 1 (a) and section 6 (b), v = 100 km/h.

a)

b)

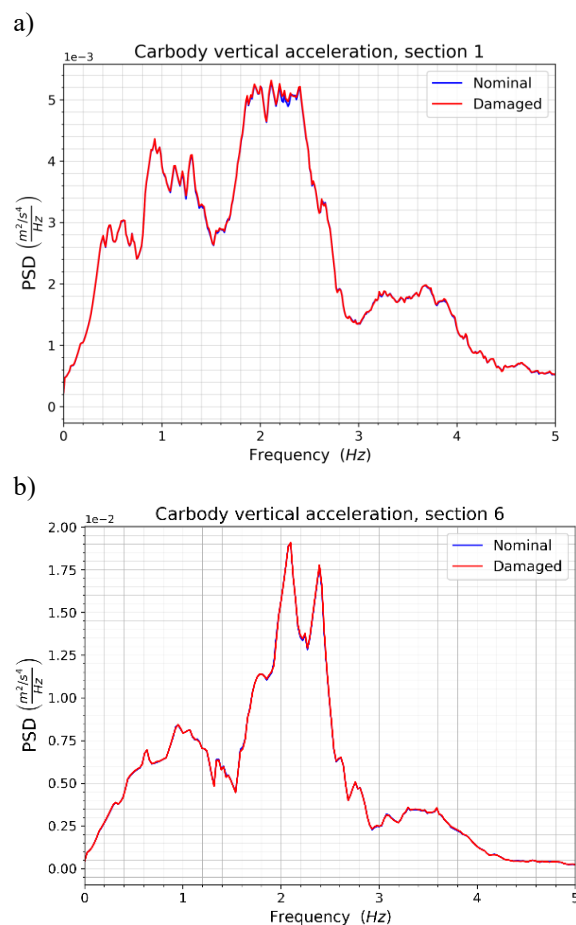

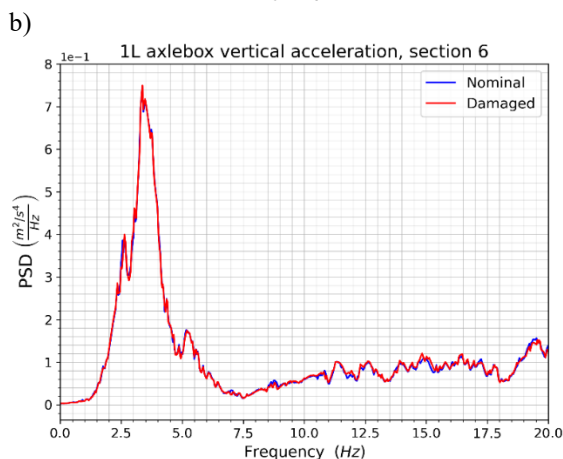Fig. 11. Carbody vertical acceleration obtained from section 1 (a) and section 6 (b), v = 100 km/h.

Fig. 12. Axlebox vertical acceleration obtained from section 1 (a) and section 6 (b), v = 160 km/h.

Fig. 13. Bogie frame vertical acceleration obtained from section 1 (a) and section 6 (b), v = 160 km/h.

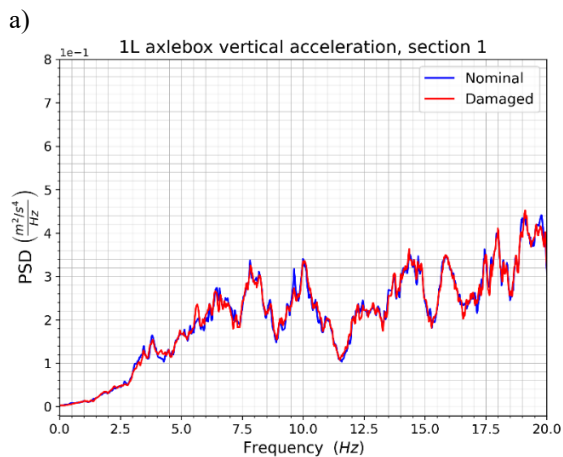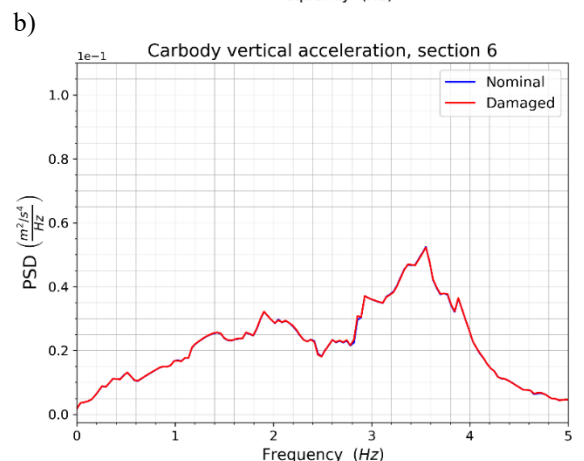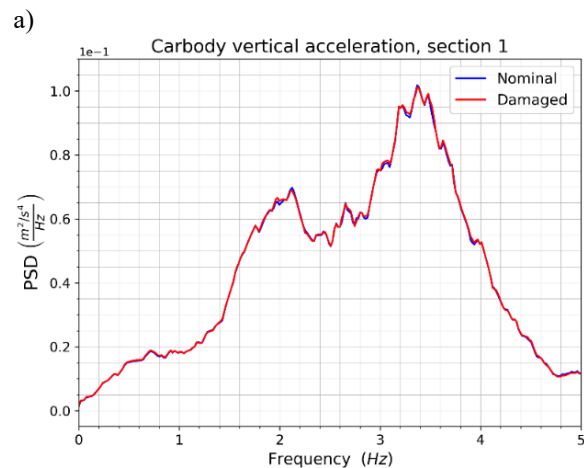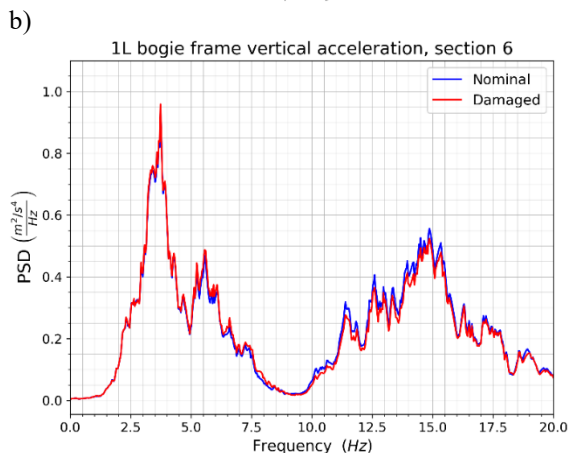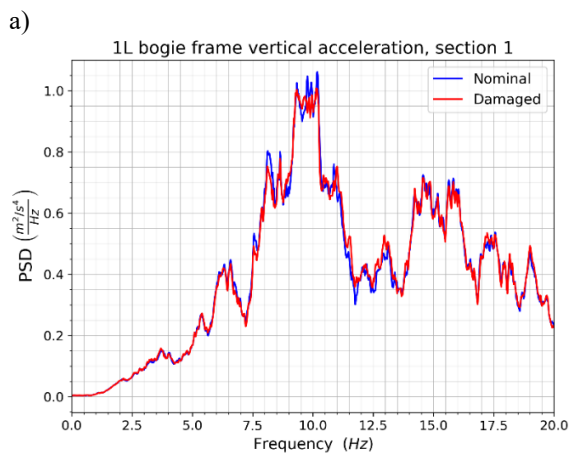Fig. 14. Carbody vertical acceleration obtained from section 1 (a) and section 6 (b), v = 160 km/h.

7. Fault detection by Artificial Neural Networks

7.1. Artificial Neural Networks configuration

This study proposes the use of artificial neural networks (ANN) to solve the problem of primary suspension damper fault detection. A typical ANN consists of three layers: input, hidden and output. When dealing with complex problems, such as image classification or speech recognition, deep neural networks (DNN) are often employed [18]. DNN is basically an ANN with multiple hidden layers between input and output layer. ANN and DNN are used in the following study for the classification problem. Due to the rail vehicle model's low sensitivity to damping detuning, it is very difficult to determine exact or even approximate magnitude of the fault. Hence, only the vehicle's condition categories have been arbitrary attributed to the considered suspension faults as depicted in Tab. 6.

Tab. 6 Condition categories attributed to the considered suspension faults.

Condition category	Attributed condition label	Fault
0.	Good condition	• All dampers nominal • 1L - 75% c_{nom} • 1L, 1R - 75% c_{nom}
1.	Minor fault	• 1L - 50% c_{nom} • 1L, 1R - 50% c_{nom}
2.	Average condition	1L - 10% c_{nom}
3.	Poor condition	1L, 1R - 10% c_{nom}
4.	Serious fault	1L - 50% c_{nom}

Condition category	Attributed condition label	Fault
		1R - 75% c_{nom}
		2L - 50% c_{nom}
		2R - 10% c_{nom}
		3L - 75% c_{nom}
		3R - 50% c_{nom}
		4L - 10% c_{nom}
		4R - 10% c_{nom}

PSD of acceleration signals fed to the neural networks have been normalised, hence there would be no discrepancy among PSD maximum values obtained from runs on tracks of different condition or different vehicles' payloads. The task for the neural network in this classification process would be extraction of relations among normalised PSD values over analysed spectrum range. In order to reduce dimensionality of input data, PSD of acceleration signals were decimated and their range reduced to 20 Hz. Data were divided into bins covering 0.22 Hz intervals. Height of the bin equals to the mean value of the samples located in the bin. One analysed file obtained from simulation contained a matrix of the resampled PSD signals of size 91 x 36, what gives 3276 nodes in the input layer.

In the process of training artificial networks, the training data consisted of matrices relating to the track sections no. 1 - 4, whereas the validating data consisted of matrices of signals acquired from section no. 6. The model was tested on data from section no. 5.

ANN were built using Keras library [11]. Three architectures of ANN were tested for suspension fault detection, namely: with one, two and three hidden layers, whose nodes number were determined by the following formula (16):

$$1st = \frac{(91 \cdot 36)}{2} = 1638$$
$$2nd = \frac{(91 \cdot 36)}{8} = 410 \qquad (16)$$
$$3rd = \frac{(91 \cdot 36)}{48} \cong 68$$

The number of the nodes of the output layer corresponds to the identified suspension conditions for the 8 simulation scenarios from Tab. 3. The outcomes of the output layer were condition categories from Tab. 4. The hidden layers neurons are activated by rectified unit activation function ($ReLu$):

$$ReLu(u) = \max(u, 0) \qquad (17)$$

Since the result of the ANN is assumed to be a categorical label, the loss function is cross entropy between label classes. The purpose of loss functions is to compute the quantity that a model should seek to minimize during training [11]. Softmax activation function, denoted hereinafter as σ, is implemented in the output layer which converts a vector of values $\boldsymbol{u}$ to a sequence of probability values, thus making it useful for multiclass classification problems [2]:

$$\sigma(\boldsymbol{u})_i = \frac{e^{u_i}}{\sum_{j=1}^{K} e^{u_j}} \qquad (18)$$

for $i = 1, \dots, K$ and $\boldsymbol{u} = (u_1, \dots, u_K) \in \mathbb{R}^K$

In the learning process of ANNs the aim is to find weights vector $\boldsymbol{w} \in \mathbb{R}^m$, what in turn can be considered as an optimization problem as defined in [8]. The optimal weights $\boldsymbol{w}^*$

$$\boldsymbol{w}^* = \arg \min_{\boldsymbol{w} \in \mathbb{R}^m} \left\{ f(\boldsymbol{w}) = \frac{1}{N} \sum_{i=1}^{N} f_i(\boldsymbol{w}) \right\} \qquad (19)$$

where: $f: \mathbb{R}^m \to \mathbb{R}$ is the loss function, f_i, for $i \in \{1, \dots N\}$,

denotes the contribution to the loss function from data point i, N denotes the total number of data points [8]. The optimization algorithm implemented for the purpose of ANN training was stochastic gradient descent [42].

8. Results of fault detection by ANNs

During training the network, the normalized results of simulation tests for both travel speeds were used combined. The validation data were the results obtained for the 6th track section. Training the network using the obtained results was difficult, and after increasing the number of epochs to 1000, a relatively low accuracy at the end of training of c.a. 0.5-0.6 was achieved. Increasing the number of epochs to over 1000 did not improve accuracy, and carried the risk of overtraining the network.

Tab. 7-9 present the results of the rail vehicle suspension condition assessment by ANNs of different configurations. Additional description is provided - if the ANN result is the same as the actual condition then it is tagged 'Match'. The tag 'Oversest.' refers to the case when the actual condition is overestimated by ANN, i.e. when the dampers faults are not as severe as they actually are (or no faults are present). Conversely, the tag 'Underest.' corresponds to the opposite condition. The accuracy is expressed as percentage of the 'Match' tags of the total number of simulation scenarios.

Tab. 7 Fault detection results by ANN of 1 hidden layer.

Scenario (Attributed condition)	Sc1 (0)	Sc2 (0)	Sc3 (1)	Sc4 (2)	Sc5 (0)	Sc6 (1)	Sc7 (3)	Sc8 (4)
ANN result	0	1	1	1	1	1	3	4
	Match	Overest.	Match	Underest.	Overest.	Match	Match	Match
Accuracy	62.5%							

Tab. 8 Fault detection results by ANN of 2 hidden layers.

Scenario (Attributed condition)	Sc1 (0)	Sc2 (0)	Sc3 (1)	Sc4 (2)	Sc5 (0)	Sc6 (1)	Sc7 (3)	Sc8 (4)
ANN result	0	0	0	1	0	0	3	4
	Match	Match	Underest.	Underest.	Match	Underest.	Match	Match
Accuracy	62.5%							

Tab. 9 Fault detection results by ANN of 3 hidden layers.

	Sc1 (0)	Sc2 (0)	Sc3 (1)	Sc4 (2)	Sc5 (0)	Sc6 (1)	Sc7 (3)	Sc8 (4)
ANN result	1	1	1	3	1	1	3	4
	Overest.	Overest.	Match	Overest.	Overest.	Match	Match	Match
Accuracy	37.5%							

The results obtained from ANNs of 1 and 2 hidden layers have the same accuracy of 62.5%, however in the case of 2 hidden layers ANN underestimated dampers condition in three scenarios: Sc3, Sc4 and Sc6. Such the incorrect assessment is unacceptable from the point of view of further exploitation and safety. Although accuracy of ANN with 3 hidden layers is the lowest, it would provide the results that are not underestimated. It generated three false alarms for the following scenarios: Sc1, Sc2 and Sc5. Nonetheless, the discrepancy was not extreme as the actual and assessed conditions were different only by one category. The selection of proper number of hidden layers and their nodes should not be based solely on the adopted measures of accuracy, or the measures should include weights favouring 'overestimated' tag (only by one category).

The accuracy values show that the ANN training for suspension fault detection is a difficult task for the assumed inputs. However, in order not to generate too many false alarms the assessments should be carried out on data obtained from more than one track section.

9. Conclusions

The suspension of a rail vehicle is a complex mechanical system whose correct online diagnosis is a difficult task due to the stochastic nature of the excitations and variable operating conditions. These excitations can cause dynamic responses of the vehicle which can mask responses due to damage of suspension components. Due to these difficulties, the paper investigated the possibility of detecting damage of primary suspension dampers using artificial neural networks. The use of neural networks was limited to damage detection and approximate assessment of the suspension condition, without indicating the exact location.

The input quantities for the proposed method are values of acceleration signals recorded identically to that used for approval testing. Thus, the method does not impose additional requirements on the measurement process and the apparatus used. In addition, the input of mass-inertia parameters and characteristics of elastic and damping elements is not required, since the method is not based on a mathematical model of the vehicle, but only on the analysis of the recorded signals.

For the tested neural network configurations and the considered faults, higher accuracy values were not achieved. In the case of the nets of 1 and 2 hidden layers, the damage was underestimated. In turn, the network with 3 hidden layers generated false alarms. However, the results of assessment by ANNs can be considered satisfactory considering the complexity of dynamic phenomena occurring in the vibration system of a rail vehicle. A possible way of decreasing number of false alarms should be sought in forming assessments made on the samples recorded on more than one track section. This approach could help mitigating random effects on acceleration signals, such as passing a railroad switch.

Further research on the use of neural networks to detect suspension faults should focus on the extension of potential faults, various states of vehicle loading, different speeds and the use of other ANN architectures, e.g. convolutional neural network. Moreover, as a part of future work, PSD measure will be expanded and should be applied to data from actual measurements from the rail vehicles.

References

1. Ankrah A A, Kimotho J K, Muvengei O M. Fusion of Model-Based and Data Driven Based Fault Diagnostic Methods for Railway Vehicle Suspension. Journal of Intelligent Learning Systems and Applications 2020; 12(03): 51–81, https://doi.org/10.4236/jilsa.2020.123004.
2. Banerjee K, C. V, Gupta R et al. Exploring Alternatives to Softmax Function: Proceedings of the 2nd International Conference on Deep Learning Theory and Applications, SCITEPRESS - Science and Technology Publications: 2021: 81–86, https://doi.org/10.5220/0010502000810086.
3. Dai L, Chi M, Guo Z et al. A physical model-neural network coupled modelling methodology of the hydraulic damper for railway vehicles. Vehicle System Dynamics 2022: 1–22, https://doi.org/10.1080/00423114.2022.2053171.
4. Dumitriu M. Condition Monitoring of the Dampers in the Railway Vehicle Suspension Based on the Vibrations Response Analysis of the Bogie. Sensors 2022; 22(9): 3290, https://doi.org/10.3390/s22093290.
5. Dumitriu M. Fault detection of damper in railway vehicle suspension based on the cross-correlation analysis of bogie accelerations. Mechanics & Industry 2019; 20(1): 102, https://doi.org/10.1051/meca/2018051.
6. EN 14363, Railway applications - Testing for the acceptance of running characteristics of railway vehicles - Testing of running behaviour and stationary tests, European Committee for Standardization, 2016.
7. ERRI B176 RP1, Preliminary studies and specifications – specification for a bogie with improved curving characteristics, Utrecht, Netherlands, 1989
8. Fjellström C, Nyström K. Deep learning, stochastic gradient descent and diffusion maps. Journal of Computational Mathematics and Data Science 2022; 4: 100054, https://doi.org/10.1016/j.jcmds.2022.100054.
9. Hayashi Y, Tsunashima H, Marumo Y. Fault Detection of Railway Vehicle Suspension Systems Using Multiple-Model Approach. Journal of Mechanical Systems for Transportation and Logistics 2008; 1(1): 88–99, https://doi.org/10.1299/jmtl.1.88.
10. http://www.ikolej.pl/zaklady-laboratoria-i-osrodki/osrodek-eksploatacji-toru-doswiadczalnego/
11. https://keras.io/api/losses/
12. Hu H, Tang B, Gong X et al. Intelligent Fault Diagnosis of the High-Speed Train With Big Data Based on Deep Neural Networks. IEEE Transactions on Industrial Informatics 2017; 13(4): 2106–2116, https://doi.org/10.1109/TII.2017.2683528.
13. Iwnicki S. Manchester Benchmarks for Rail Vehicle Simulation. Vehicle System Dynamics 1998; 30(3–4): 295–313, https://doi.org/10.1080/00423119808969454.
14. Kalker J J. A Fast Algorithm for the Simplified Theory of Rolling Contact. Vehicle System Dynamics 1982; 11(1): 1–13, https://doi.org/10.1080/00423118208968684.
15. Karlsson H, Qazizadeh A, Stichel S, Berg M. Condition Monitoring of Rail Vehicle Suspension Elements: A Machine Learning Approach. In Klomp M, Bruzelius F, Nielsen J, Hillemyr A (eds): Advances in Dynamics of Vehicles on Roads and Tracks, Cham, Springer International Publishing: 2020: 119–127, https://doi.org/10.1007/978-3-030-38077-9_14.
16. Konowrocki R, Chojnacki A. Analysis of rail vehicles' operational reliability in the aspect of safety against derailment based on various methods of determining the assessment criterion. Eksploatacja i Niezawodnosc - Maintenance and Reliability 2019; 22(1): 73–85, https://doi.org/10.17531/ein.2020.1.9.
17. Konowrocki R, Kalinowski D, Szolc T, Marczewski A. Identification of safety hazards and operating conditions of the low-floor tram with independently rotating wheels with various drive control algorithms. Eksploatacja i Niezawodnosc - Maintenance and Reliability 2021; 23(1): 21–33, https://doi.org/10.17531/ein.2021.1.3.
18. Kouretas I, Paliouras V. Simplified Hardware Implementation of the Softmax Activation Function. 2019 8th International Conference on Modern Circuits and Systems Technologies (MOCAST), Thessaloniki, Greece, IEEE: 2019: 1–4, https://doi.org/10.1109/MOCAST.2019.8741677.
19. Kraemer P, Friedmann H, Richter M. Vibration-based damage identification on the suspension of a railway waggon – Findings from snap-back experiments with transient excitation. International Journal of Rail Transportation 2020; 8(4): 387–400, https://doi.org/10.1080/23248378.2019.1675190.

20. Li P, Goodall R, Weston P et al. Estimation of railway vehicle suspension parameters for condition monitoring. Control Engineering Practice 2007; 15(1): 43–55, https://doi.org/10.1016/j.conengprac.2006.02.021.
21. Li P, Goodall R. Model based condition monitoring for railway vehicle systems. Control 2004, University of Bath, 2004, ID-508.
22. Liu X Y, Alfi S, Bruni S. An efficient recursive least square-based condition monitoring approach for a rail vehicle suspension system. Vehicle System Dynamics 2016; 54(6): 814–830, https://doi.org/10.1080/00423114.2016.1164869.
23. McConville J B, McGrath J F. Introduction to ADAMS theory. Ann Arbor, Michigan, USA, Mechanical Dynamics, Inc.: 1998.
24. Mei T X, Ding X J. Condition monitoring of rail vehicle suspensions based on changes in system dynamic interactions. Vehicle System Dynamics 2009; 47(9): 1167–1181, https://doi.org/10.1080/00423110802553087.
25. Melnik R, Kostrzewski M. Rail Vehicle's Suspension Monitoring System - Analysis of Results Obtained in Tests of the Prototype. Key Engineering Materials 2012; 518: 281–288, https://doi.org/10.4028/www.scientific.net/KEM.518.281.
26. Melnik R, Koziak S. Rail vehicle suspension condition monitoring – approach and implementation. Journal of Vibroengineering 2017; 19(1): 487–501, https://doi.org/10.21595/jve.2016.17072.
27. Mitschke M. Dynamik der Kraftfahrzeuge. B: Schwingungen. 2., völlig neubearb. Aufl. Berlin Heidelberg, Springer: 1984.
28. Petrović D, Atmadzhova D, Bižić M. Advantages of installation of rubber-metal elements in suspension of railway vehicles. Split, Croatia, University of Zagreb: 2014; Road and Rail Infrastructure III: 491–497.
29. Ren J, Jin W, Li L et al. Performance Degradation Estimation of High-Speed Train Bogie Based on 1D-ConvLSTM Time-Distributed Convolutional Neural Network. Computational Intelligence and Neuroscience 2022; 2022: 1–16, https://doi.org/10.1155/2022/5030175.
30. Sakellariou J S, Petsounis K A, Fassois S D. Vibration based fault diagnosis for railway vehicle suspensions via a functional model based method: A feasibility study. Journal of Mechanical Science and Technology 2015; 29(2): 471–484, https://doi.org/10.1007/s12206-015-0107-0.
31. Same M H, Gandubert G, Gleeton G et al. Simplified Welch Algorithm for Spectrum Monitoring. Applied Sciences 2020; 11(1): 86, https://doi.org/10.3390/app11010086.
32. Sorribes-Palmer, Felix, Luber, Bernd, Fuchs, Josef et al. Data-driven fault diagnosis of bogie suspension components with on-board acoustic sensors. 2020; 5(1): 13.
33. UIC 518, Testing and approval of railway vehicles from the point of view of their dynamic behaviour – Safety – Track fatigue – Ride quality. International Union of Railways (UIC) Leaflet, 2009.
34. Wang W L, Zhou Z R, Yu D S et al. Rail vehicle dynamic response to a nonlinear physical 'in-service' model of its secondary suspension hydraulic dampers. Mechanical Systems and Signal Processing 2017; 95: 138–157, https://doi.org/10.1016/j.ymssp.2017.03.031.
35. Wei X, Guo K, Jia L et al. Fault Isolation of Light Rail Vehicle Suspension System Based on D-S Evidence Theory and Improvement Application Case. Journal of Intelligent Learning Systems and Applications 2013; 05(04): 245–253, https://doi.org/10.4236/jilsa.2013.54029.
36. Wei X, Jia L, Liu H. Data-driven fault detection of vertical rail vehicle suspension systems. Proceedings of 2012 UKACC International Conference on Control, Cardiff, United Kingdom, IEEE: 2012: 589–594, https://doi.org/10.1109/CONTROL.2012.6334696.
37. Welch P. The use of fast Fourier transform for the estimation of power spectra: A method based on time averaging over short, modified periodograms. IEEE Transactions on Audio and Electroacoustics 1967; 15(2): 70–73, https://doi.org/10.1109/TAU.1967.1161901.
38. Wu Y, Jin W, Ren J, Sun Z. Fault Diagnosis of High-Speed Train Bogie Based on Synchrony Group Convolutions. Shock and Vibration 2019; 2019: 1–13, https://doi.org/10.1155/2019/7230194.
39. Ye Y, Huang P, Zhang Y. Deep learning-based fault diagnostic network of high-speed train secondary suspension systems for immunity to track irregularities and wheel wear. Railway Engineering Science 2022; 30(1): 96–116, https://doi.org/10.1007/s40534-021-00252-z.
40. Zboinski K, Golofit-Stawinska M. Investigation into nonlinear phenomena for various railway vehicles in transition curves at velocities close to critical one. Nonlinear Dynamics 2019; 98(3): 1555–1601, https://doi.org/10.1007/s11071-019-05041-2.
41. Zeng Y C, Song D L, Zhang W H et al. Stochastic failure process of railway vehicle dampers and the effects on suspension and vehicle dynamics. Vehicle System Dynamics 2021; 59(5): 703–718, https://doi.org/10.1080/00423114.2019.1711136.
42. Zhou B, Han C, Guo T. Convergence of Stochastic Gradient Descent in Deep Neural Network. Acta Mathematicae Applicatae Sinica, English Series 2021; 37(1): 126–136, https://doi.org/10.1007/s10255-021-0991-2.
43. Zoljic-Beglerovic S, Stettinger G, Luber B, Horn M. Railway Suspension System Fault Diagnosis using Cubature Kalman Filter Techniques. IFAC-PapersOnLine 2018; 51(24): 1330–1335, https://doi.org/10.1016/j.ifacol.2018.09.562